Palaeomagnetism, magnetic fabrics and the structural style of the Hornelen Old Red Sandstone, Western Norway

T. H. TORSVIK, B. A. STURT, D. M. RAMSAY, et al.

Journal of the Geological Society 1988; v. 145; p. 413-430
doi: 10.1144/gsjgs.145.3.0413

Journal of the Geological Society, London, Vol. **145,** 1988, pp. 413–430, 19 figs, 3 tables. Printed in Northern Ireland

Palaeomagnetism, magnetic fabrics and the structural style of the Hornelen Old Red Sandstone, Western Norway

T. H. TORSVIK,[1]* B. A. STURT,[2] D. M. RAMSAY,[3] D. BERING[4] & P. R. FLUGE[5]

[1] *Department of Earth Sciences, University of Oxford, Oxford OX1 3PR, UK*

[2] *Geological Survey of Norway, P.O. Box 3006, N-7001 Trondheim, Norway*

[3] *Department of Geology, University of Dundee, Dundee DD1 4HN, UK*

[4] *Institute of Geology, University of Bergen, N-5000 Bergen, Norway*

[5] *Institute of Geophysics, University of Bergen, N-5000 Bergen, Norway*

Abstract: The Old Red Sandstone of the Hornelen district, western Norway, forms part of a major fold-terrane, and the principal magnetization is associated with the Late Devonian to Early Carboniferous Svalbardian/Solundian Orogeny. The present fault margins of the Hornelen Massif, claimed by various authors to represent subordinate Devonian splay faults associated with megashearing in the North Atlantic or lateral ramps in a regional extensional tectonic setting, are shown to be post-Devonian structures, and the present outline of the Hornelen Massif is a Mesozoic (Jurassic) 'graben'.

The Hornelen Old Red Sandstone (ORS) is the largest of the Devonian massifs in Norway (Fig. 1), and comprises *c.* 25 km of mainly axially-deposited alluvial grey sandstones and siltstones interfingering with marginal fan-conglomerates (Steel *et al.* 1985). Plant and fish fossils found in the upper part of the succession indicate an upper Lower Devonian age. The great apparent stratigraphical thickness, alluvial sedimentation and basin asymmetry, together with repetitions of basin-wide, upward-coarsening sequences associated with lateral extension, were among the factors that led Bryhni (1964, 1978) and Steel and co-workers (see review in Steel *et al.* 1985) to the conclusion that the Hornelen 'Basin' was tectonically generated. The basin developed with a principal component of hinge-faulting or dextral oblique shear along, or close to, the present northern marginal fault (Figs 1b & 2). Depocentres were considered to have migrated eastwards with time, in an opposite direction to the palaeoflow indicators. Over much of the outcrop of the Devonian sediments there are few penetrative effects of deformation. The rocks abound in sedimentary structures, and primary features, such as bedding, dominate the outcrop pattern. Megascopic cleavage is either absent or difficult to identify and can only be observed as a well developed structure at a few localities, particularly in the north-eastern and western parts of the massif.

The Devonian deposits unconformably overlie a basement of Cambro-Silurian greenstones in the west and granodiorite/quartzites to the north-west, while the southern and northern margins of the massif are marked by moderate- to high-angle faults. Pebbles in conglomerates along the southern margin of the Devonian outcrop are identified as coming from the surrounding Precambrian meta-anorthosites/gneisses, which belong to the Møre Window of the Western Gneiss Region. In the north, conglomerate clast provenance is less clear (Steel & Gloppen 1980). The eastern margins of the Western Norwegian Devonian sedimentary developments are commonly depicted as thrusts (Bryhni 1964), but have recently been re-evaluated as major syn-depositional listric normal faults (Hossack 1984). In this novel extensional model, collapse of the footwall, i.e. the Måløy Fault (Hossack 1984) or Nordfjord-Sogn detachment (Norton 1986), is considered to have led to sedimentary deposition in the hanging wall. Eastward onlap relationships originated as a roll-over anticline which accompanied the listric faulting. In Hossack's model E–W folding and low-grade metamorphism of the Devonian sediments were produced as an accommodation to the lateral ramps produced by the presently observed marginal faults, with the implication of a syn-kinematic extensional origin for both deposition and deformation.

The Kvamshesten and in part the Solund Massifs are undoubtedly floored by low-angle faults, but most likely of post-depositional origin (Torsvik *et al.* 1986, 1987*b*; Ramsay *et al.* 1987). The Devonian substrate in the Hornelen area indeed contains zones of mylonitic rocks (Brynhi 1964), but to date, no definitive geological evidence for a syn-depositional *Devonian* low-angle fault along the eastern margin has been documented. The area concerned is an area of geological complexity and has physical access problems. At least part of the eastern margin is a surface of unconformity (Fig. 2), and any displacement was insufficient to produce significant mylonitization or destruction of well-preserved ORS weathering profiles in the substrate (Ramsay *et al.* 1987). The Hornelen Devonian sediments are assumed by most authors to have formed in an almost *in situ* basin where the original basin margins were approximately those seen today. In detail the pattern is more complex and the facies belts are sharply truncated by the northern and southern marginal faults. The present authors opine that these faults are substantially later in formation than the ORS deposition and we will discuss our reasoning for this.

* Present address: Geological Survey of Norway, P.O. Box 3006, N-7001 Trondheim, Norway.

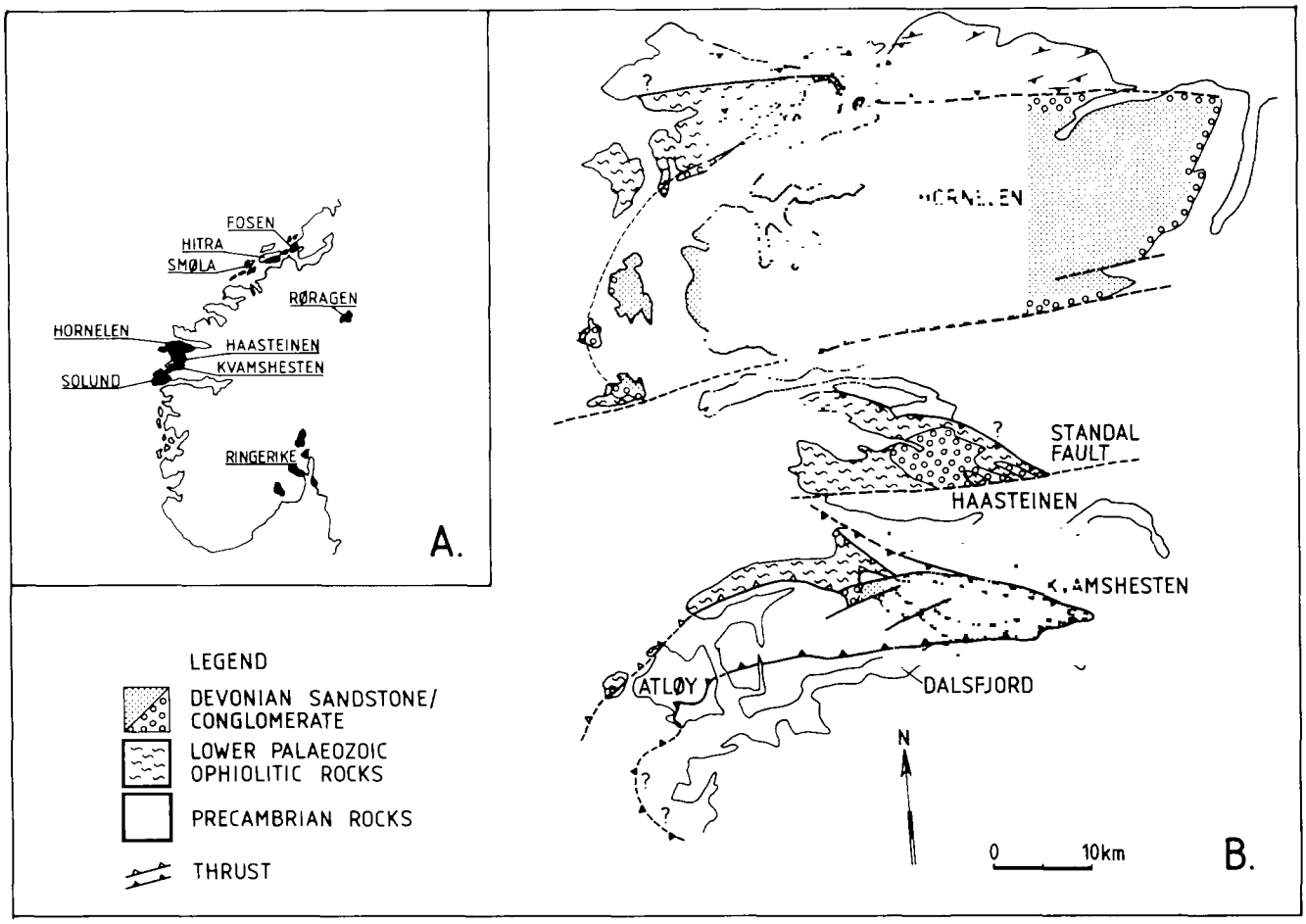

Fig. 1. (**A**) Geographic location of Old Red Sandstone deposits in Norway, (**B**) geological sketch map of the Kvamshesten, Håsteinen and Hornelen area (modified from Roberts (1983) and Torsvik *et al.* (1987*a*)). The pattern of foliations near the northern margin of the Hornelen Massif is simplified from Bryhni (1966).

Sampling and the magnetic fabric

The anisotropy of magnetic susceptibility (AMS, K) was measured for 330 samples from a total of 45 sites (Fig. 2; cf. Table 1; site numbers are not sequentially listed) with a low field induction bridge (KLY-1). The Devonian substrate was examined close to the margins of the Hornelen Massif, two of the sites (23 & 25) having previously been sampled (Torsvik *et al.* 1987*a*). The degree of anisotropy (%An = (P2 − 1)/100) is generally twice or three times that recorded in the Devonian sediments (Fig. 3), and the shapes of the magnetic susceptibility ellipsoids from basement samples are all oblate (Fig. 4a). Notably low anisotropies in the substrate, however, are recorded in fractured and brecciated gneisses close to the northern marginal fault (cf. site 32). Close to the fault (<2–3 m), the magnetic foliation ($K_{max} - K_{int}$) dips steeply to moderately southwards and trends approximately parallel to this structure, with near E–W subhorizontal lineations (K_{max}; Fig. 2). North of the massif, however, the megascopic gneissic foliation has a more north-easterly trend, which is oblique to the fault-margin, and defines an antiformal structure (Fig. 1b; cf. fig. 1 in Bryhni 1966). Mylonitic Precambrian meta-anorthosites from south of the massif (site 25) have anisotropies as high as 42%. There is an apparent decrease in anisotropy and oblate flattening strain toward the southern marginal fault (cf. Figs 2–4). Subhorizontal to intermediately plunging magnetic lineations vary from NE to SE, and a relatively tight antiformal structure of the pre-Devonian magnetic foliation is indicated (Fig. 2). The magnetic fabrics in both Palaeozoic and Precambrian basement rocks closely relate to field-observed planar and linear fabrics, and magnetic lineations plunge to the east (Fig. 5g). Apart from site 20, the distribution of site means of K_{min} and the poles to observed foliation define an approximately N–S girdle, with an average easterly plunge of 15–20° (Fig. 5d).

In the Devonian sediments, large variations in anisotropy (3–15%) and shape of the magnetic ellipsoids between sites partly reflect differences in lithology (Figs 3 & 4b). The majority of sites have oblate magnetic ellipsoids, although prolate ellipsoids are occasionally developed along the primary western contact, i.e. the structurally lowest beds. Compressional strains, attended by the development of megascopic cleavage, are reflected most notably along the western margin and in the steeply dipping beds, *in part inverted* (e.g. site 2; cf. Fig. 2), in the north-eastern corner of the massif. Along the western unconformity the cleavage is largely confined to the more fine-grained lithologies.

Distribution of K_{min} tends to be close to the poles of

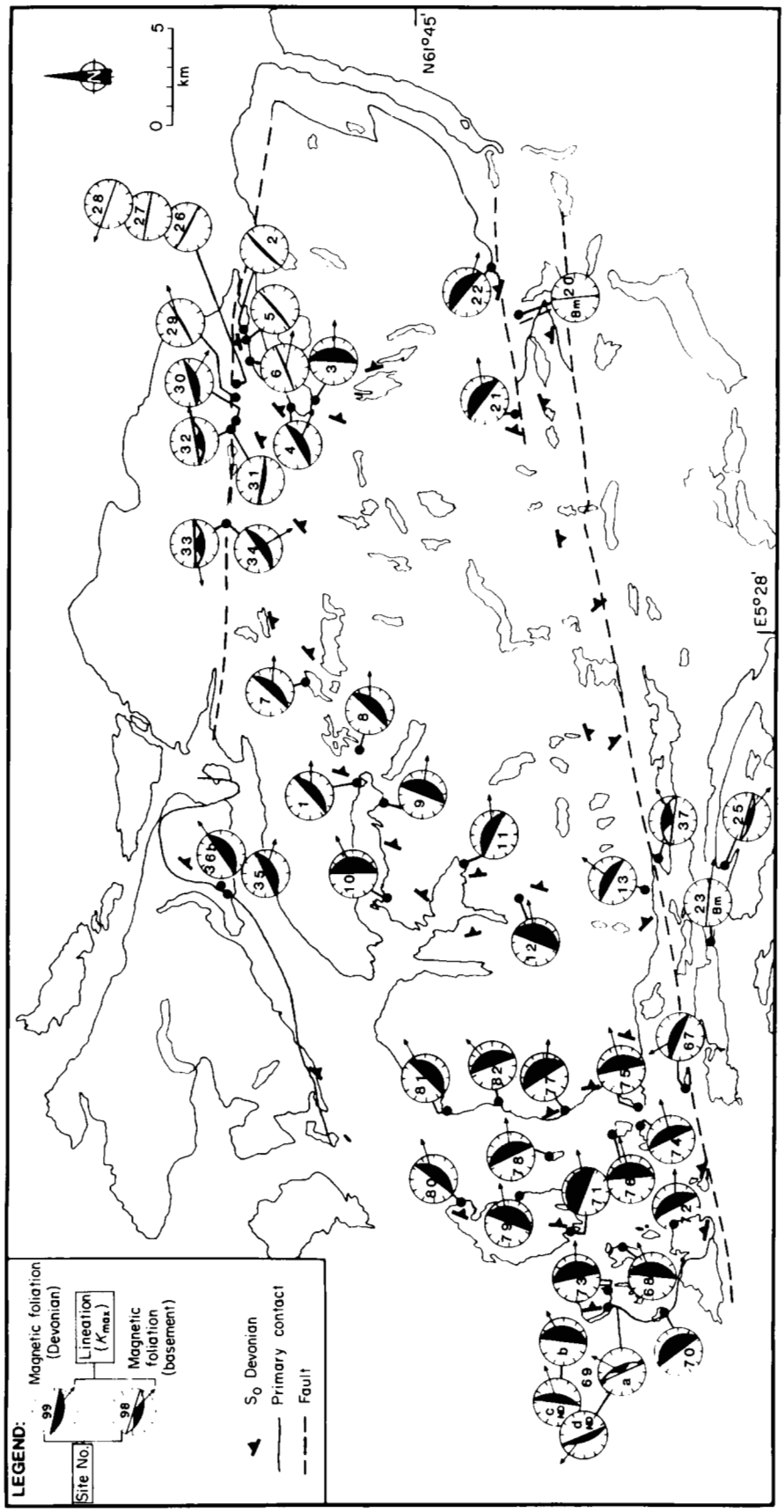

Fig. 2. The magnetic fabrics and sampling points in the Hornelen Massif and substrate. The magnetic foliation and lineation are plotted as downward-dipping planes (lower hemisphere equal angle stereographic projection) and plunges, respectively. See legend and text for details.

Table 1. *Site-mean statistics* (in situ)

Site	Lithology		Dec.	Inc.	α_{95}	Polarity N	Polarity R	S_0 (strike°/dip°)	RGr
Devonian rocks									
1	Grey SST		135	−3	8	—	5	013/31	?
2	Grey SST	[LB]	060	+69	18	3	—	222/82(i)	B
			057	+7	11	4	1		A
3	Grey SST		072	+13	10	5	—	010/28	A
4	Grey SST	[LB]	356	+60	10	4	1	042/48	B
5	Grey SST	[LB]	354	+46	36	2	—	051/82	B
6	Grey SST	[LB]	014	+52	14	2	—	055/86	B
7	Grey SST	No successfully tested samples						039/43	
8	Grey SST		212	+35	8	—	7	036/32	A
9	Grey SST		190	+27	15	—	2	023/28	A
10	Grey SST	No successfully tested samples						040/25	
11	Grey SST	No successfully tested samples						350/27	
12	Grey SST	No successfully tested samples						020/24	
13	Grey SST		225	−39	11	3	4	275/47	B
21	Red SST/SILT		227	+21	12	2	6	093/40	A
22	Grey SILT		026	+50	18	4	—	330/28	B
26								252/82(i)	
27	BRECCIA		312	+63	10	6	—	252/82(i)	B
28								100/87	
29	Grey SST		004	+64	15	4	—	093/75	B
			045	−22	25	4	1		A
30	Grey SILT		215	+42	14	—	5	079/70	A
31	Grey SILT	NRM intensity < noise level						081/75	
34	Red SILT	Cf. Fig. 13 and text						052/73	
35	Grey SILT	Smeared distribution of ChRc						064/62	
36b	Grey SST		248	+1	20	—	4	045/40	A
67	Grey SST		184	+25	9	1	1	300/54	A
68	Grey pebbly SST		188	−52	11	5	5	354/18	B
69	Red SST, N. Dykes		058	+53	16	5	3	349/28	B
	Neptunian Dykes		051	−7	14	5	—		A
70	Red SILT	No successfully tested samples						342/28	
71	Grey SST/SILT		204	+9	25	—	3	017/23	A
72	Grey SST		015	−9	35	2	—	325/49	A
73	Grey SST		237	+34	6	—	3	000/20	A
74	Grey SST	[LB]	007	+45	10	6	—	010/20	B
75	Grey SST/SILT		193	+16	18	1	5	011/22	A
76	Grey SST/SILT		049	−18	10	4	—	005/20	A
77	Grey SST/SILT		194	+13	18	3	4	325/20	A
78	Grey SST/SILT		221	−35	16	—	3	334/23	B
			227	+24	19	1	5		A
79	Grey SST/SILT		017	−20	11	8	—	358/20	A
80	Grey SST/SILT	[LB]	172	+6	8	1	3	028/26	?
			220	+36	27	—	3	028/26	A
81	Grey SST		234	+21	25	—	3	024/28	A
82	Grey SST/SILT		322	−3	9	3	—	002/25	?
Pre-Devonian Rocks									
20	Phyllite	[LB]	187	−41	8	—	5		B
23	Anorthosite	[LB]	249	−55	5	—	6		B
25	Anorthosite		225	+14	17	6	3		A
32	Gneiss	Smeared distribution of ChRc							
33	Gneiss	Smeared distribution of ChRc							
36	Granodiorite	NRM below instrumental noise level							
37	Gneiss	No successfully tested samples							
69a	Greenstone	Smeared distribution of ChRc (cf. Fig. 12)							

SST, sandstone; SILT, siltstone; [LB], low blocking component (<250–350 °C); Dec, mean declination; Inc, mean inclination; α_{95}, 95% confidence circle (Fisher 1953); Polarity (number of specimens): N, normal; R, reverse; S_0, bedding (Devonian); RGr, remanence group classification; (i) indicates inverted stratigraphy.

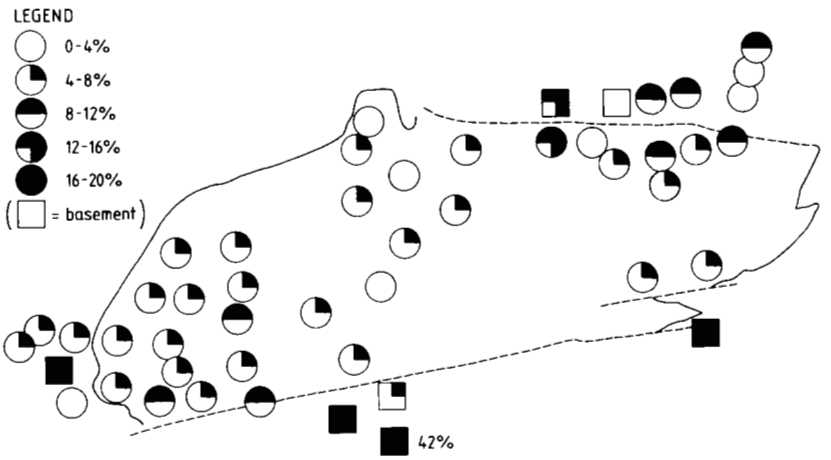

Fig. 3. Variation in the degree of magnetic susceptibility anisotropy. Positions of symbols correspond to stereographic plots in Fig. 2.

bedding and cleavage (compare Figs 5a–c); thus, the magnetic foliation planes shown in Fig. 2 principally outline the pre-eminent fold style of the massif, i.e. a major synclinal structure with a subordinate aniticline and syncline (Grøndalen) close to the southern margin. A strong E–W magnetic lineation (Figs 2 & 5e), sub-parallel to the principal axial direction of sediment transport, may initially suggest a purely primary/compactional and folded magnetic foliation, with the lineation mirroring the palaeocurrent pattern. This may indeed apply to some of the sites, but this is an over-simplification. The magnetic lineations, at least in part, appear to be controlled by a tectonic fabric. Easterly plunging magnetic lineations are subparallel to fold-axes and correspond to both magnetic and tectonic lineations in the basement (Figs 5e & g). Similar features characterize the Håsteinen and Kvamshesten areas (Torsvik *et al.* 1986, 1987*a*), where lineations are either intersection (S_0/S_1) or stretching types. The spatial distribution of the magnetic lineations throughout the Hornelen Massif is consistently more E–W than the palaeocurrent estimates. For example, palaeocurrents trend mostly N–S in the NW part of the Massif (see fig. 5 in Bryhni 1978) in contrast to the very consistent E–W magnetic lineation pattern. Nilsen (1968) also demonstrated that pebble-lineations recorded in the Solund Massif are much more consistent than cross-bedding data, coinciding with a tectonic lineation close to the southern margin of that massif. The magnetic fabrics recorded from some Neptunian dykes on Batalden (Site 69; Fig. 2) partly correspond to the general magnetic fabric pattern in the Devonian sediments of the Massif, and notably with the magnetic fabric pattern of lower Palaeozoic basement rocks (compare sites 69a–c in Fig. 2), and are unlikely to represent primary fabrics. Also the degree of apparent flattening strain appears to decrease down-section, indicating that pure diagenetic compaction is unlikely to have controlled the magnetic fabrics (Fig. 4b).

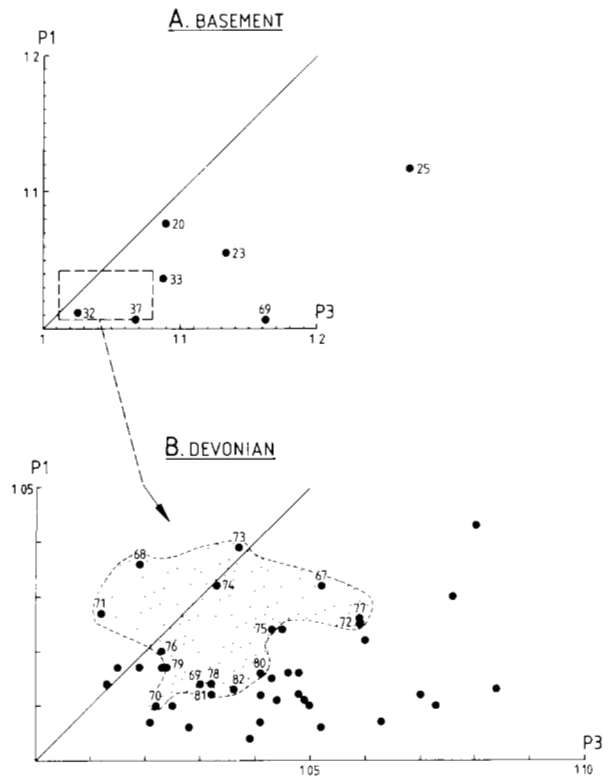

Fig. 4. Flinn diagrams for the substrate (**A**) and the Devonian samples (**B**). P1 (K_{max}/K_{int}) and P3 (K_{int}/K_{min}) represent lineation and foliation, respectively. Stippled area in (**B**) corresponds to sampling sites along the western, primary unconformity, which tend to show a smeared distribution into the apparent prolate field in the Flinn diagram. Rectangular area in (**A**) corresponds to the part of the Flinn diagram occupied by the Devonian data.

K_{min} and the poles to S_0 and S_1 in the Devonian define near coincident girdles with a general N–S orientation (Fig. 5a–c) and an average easterly plunge of *c.* 15°. This closely compares with the somewhat more strongly folded substrate, and indicates N–S compression. A cautious inspection of the differences in the plunges of K_{min} and pole to S_0 (Fig. 6) discloses a pattern of magnetic foliations which are close to (±5°), or somewhat more steeply inclined than, the bedding. The latter may indicate the influence of a cleavage development during folding of the Devonian sediments (sites with inverted bedding, e.g. site 2, are also inverted in the diagram for reasons of simplicity in the discussion). Note that some sites with definite development of an axial plane cleavage show larger deviation in strike of the magnetic foliation (e.g. sites 71, 11) than in dip. The overall impression, however (Figs 2, 5 & 6), indicates that both the magnetic *foliation* and megascopic cleavage predominantly have a pre-fold origin. Some sites deviate from this pattern, but these are preferentially located close to the

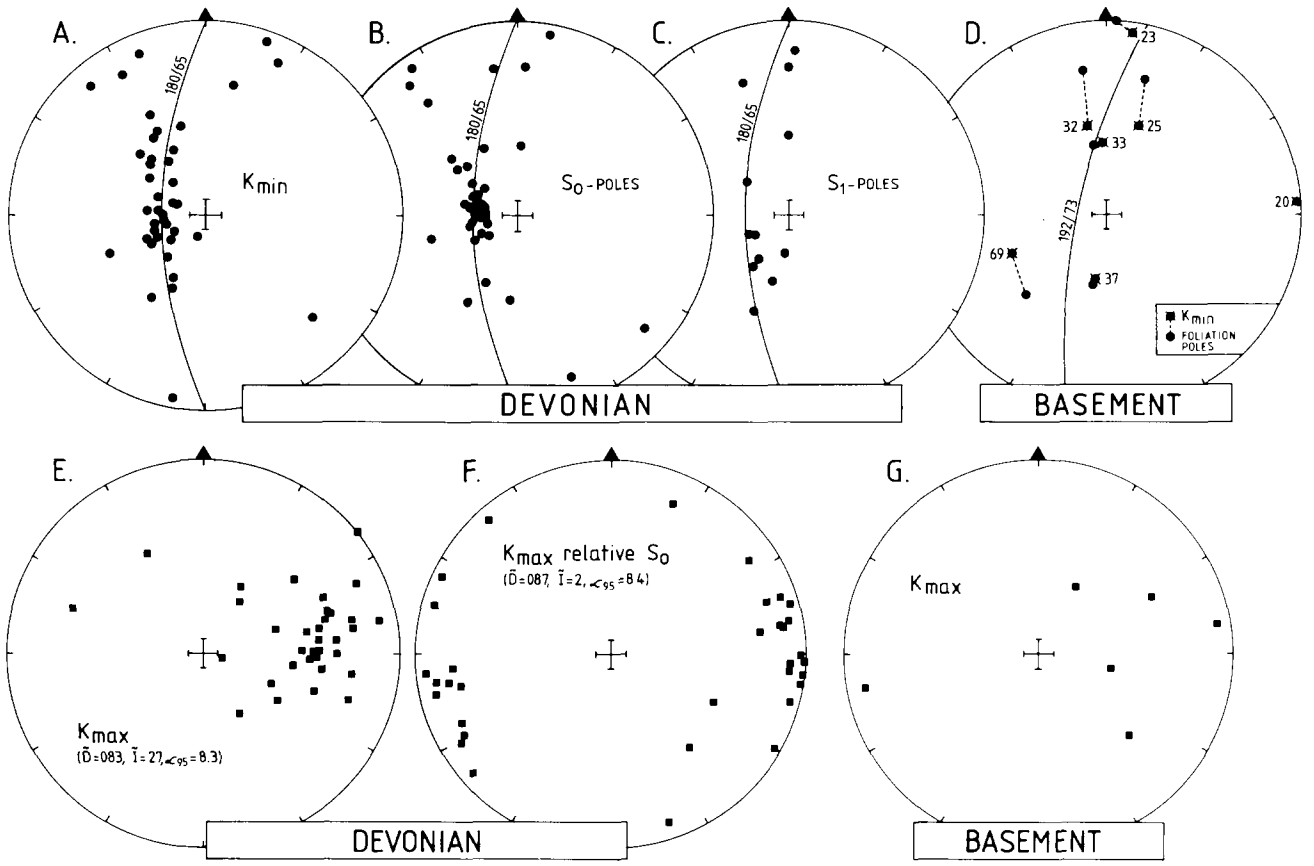

Fig. 5. Distribution of K_{min} **(A)**, S_0 **(B)** and S_1 **(C)** from the Devonian sediments and comparison of K_{min} and observed poles to foliation planes in the substrate **(D)**. **(E)** and **(F)** show K_{max} (Devonian) in *in situ* coordinates and relative to S_0, respectively, and K_{max} recorded from the substrate are shown in **(G)**. Note that all data represent site-mean values (based on 5–15 observations from each site). Equal angle stereographic projections.

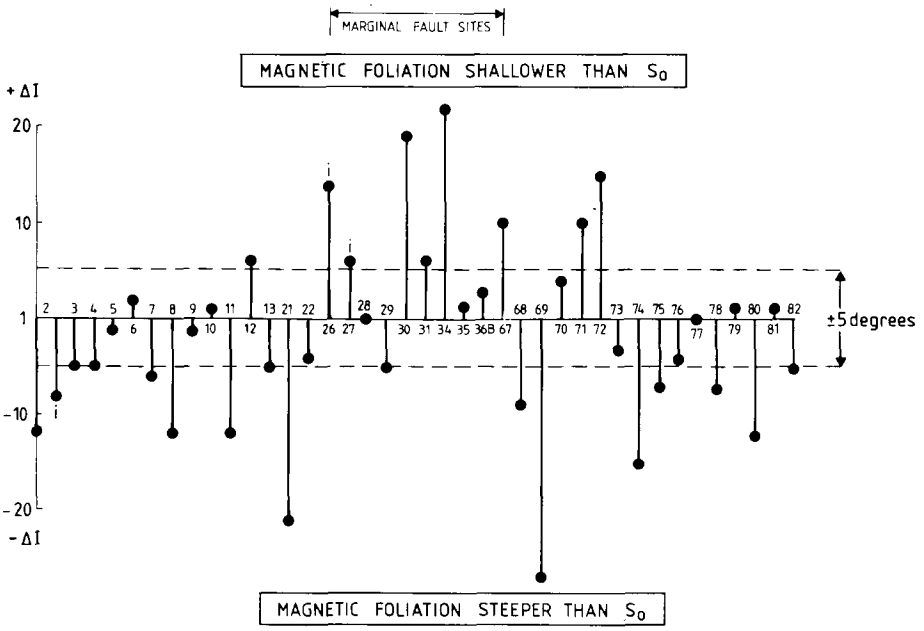

Fig. 6. The angular difference in *dip* ΔI between K_{min} and poles to S_0. Negative values correspond to a magnetic foliation which is more steeply inclined than the bedding. Data from sites with inverted stratigraphy are inverted also in the diagram for reasons of simplicity and labelled '*i*'. Numbers (horizontal axis) denote sampling site number.

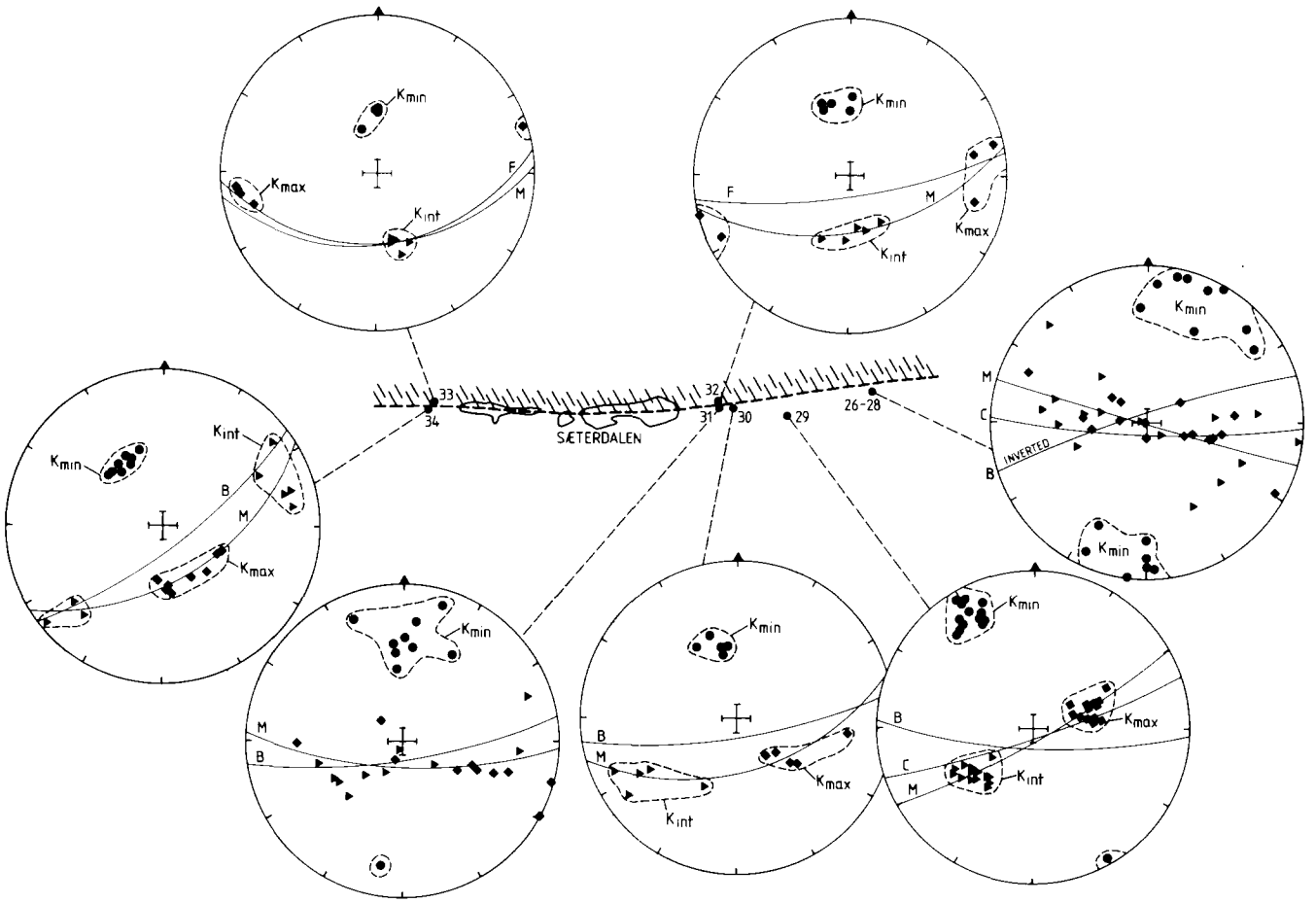

Fig. 7. Details of the magnetic fabrics along the northern marginal fault. Downward dipping great circles denoted by M, C, B and F correspond to magnetic foliation, cleavage, bedding (Devonian) and foliation (i.e. the fault-contact plane) in the contact gneisses.

northern marginal fault (e.g. sites 26 & 27 and 30–31 & 34). Details of the magnetic fabrics from sites 26–34, generally within 10 m of the contact, are shown in Fig. 7. Precambrian gneisses and Devonian sediments both exhibit a moderate to steeply southward-dipping magnetic foliation, which corresponds to the observed cleavage at some sites, and the magnetic foliation together with the fault-plane orientation intersects bedding at a slightly shallower angle. Apart from site 34 where the magnetic foliation and bedding are oblique to the fault (see next section), it is evident that the magnetic fabrics in both the gneiss and the contact sediments close to the northern marginal fault mirror a post-fold and fault-plane orientated fabric.

The unconformity in the NW part of the Massif was investigated at sites 35 and 36, and cores from site 36 were partly drilled through the unconformity. The rheologically competent granodioritic rocks of the substrate are homogeneous and isotropic in fabric. In contrast, a similar granodiorite located to the east of the Solund Massif is strongly mylonitic (Kolderup 1926; Mikkelsen 1986). For palaeomagnetic purposes only two Devonian sites near the eastern margin were tested. Sites 21 and 22 (Fig. 2) were located close to a fault parallel to the southern marginal fault and a primary unconformity, respectively. The magnetic foliations from both sites are substantially bedding-parallel, but are influenced by an axial-plane cleavage, notably site 21 (cf. Fig. 6), which has a near easterly lineation. The immediate substrate, site 20 (Fig. 2), discloses a steeply dipping magnetic foliation trending N–S, a trend which is incompatible with the regional metamorphic foliation pattern.

Palaeomagnetic experiments

Stepwise thermal or alternating field (AF) demagnetizations were fulfilled for 294 and 47 samples, respectively (Figs 8–14). Characteristic remanance components (ChRc) obtained from numerical estimates of linear segments in vector diagrams (Kent *et al.* 1983; Torsvik 1986), indicate a complex pattern (Fig. 15a), but interpretation and analysis of individual sites indicates a pattern of two major remanence components, both having a dual polarity structure (Fig. 15b, Tables 1 & 2), denoted A and B.

Remanence A is characterized by south-westerly declinations, with mostly downward-pointing inclinations, or north-easterly declinations with upward-pointing inclinations. Exemplary single component A remanences are recognized from a number of sites (cf. Fig. 8a), together with reasonable within-site grouping. Samples from other A component sites disclose a somewhat more irregular decay pattern (Fig. 8b), but indicate essentially 'noisy' single-component remanence. Usually thermal demagnetization

Table 2. *Overall palaeomagnetic data*

	Dec.	Inc.	N	α_{95}	k	Pole (°) Lat	Long	dp/dm
Group A (Devonian)								
In situ:	218	20	20	9.35	11.2			
20% unfolded:	216	21	20	9.22	11.54	N12	E147	5/10
100% unfolded:	210	25	20	12.35	6.42			
Group B (Devonian)								
In situ:	020	54	12	10.9	13.8	[N60	E151	11/15]
100% unfolded:	077	40	12	24.7	2.7			
Group B (Devonian and basement)								
In situ:	022	54	14	10.1	13.7	N59	E148	10/14

N, number of sites; k, precision parameter; Pole: Lat, latitude; Long, longitude; dp/dm, semi-axis of the oval of 95% confidence about the mean pole.

See Table 1 for further explanation.

was not successful in reducing the NRM intensity by more than 25–50% at temperatures around 500 °C. This is due to pronounced viscous behaviour at higher temperatures, due to (1) pyrrhotite inverting to magnetite at temperatures around 350–450 °C and/or (2) reduction of hematite at temperatures around 500–600 °C presumably owing to the presence of modest amounts of organic material in the sediments. Judging from the thermal blocking spectra, thermomagnetic analysis (cf. Figs 14a–c), isothermal remanent magnetization (Fig. 14d) and AF demagnetization decay curves, the bulk magnetic properties of the Devonian specimens are governed by magnetite, hematite and pyrrhotite in decreasing order of importance. The NRM intensity typically varied between 10 and 30 mA m^{-1}, though large within-site variations (magnetic inhomogeneities) were observed, with NRM intensities as high as 500 mA m^{-1}. It is difficult to point to systematic differences in the bulk magnetic properties between normal and reverse sample directions. However, there is a *general impression* that samples with typical blocking temperatures exceeding 600 °C are of reverse polarity, whereas most normal polarity data are within the 'magnetite' range (compare Figs 8a & b). In the case of dual-polarity remanances, the reverse components most commonly occupy the high-blocking spectra.

The A component frequently co-exists with the B remanence, which is steeply inclined with declinations near NNE–SSW. In certain examples, typical of almost all tested substrate samples, the B remanence was identified (Figs 9a & b) as a low blocking component in the NRM-250/350 °C range, whereas the top component remained unidentified due to pronounced viscous behaviour at higher temperatures and/or NMR dropping below instrumental noise level (pronounced off-origin trace). Incidentally, the B remanance may totally dominate the NRM (Fig. 9c; single-component nature). Substantial overlap in the blocking spectra may exist between the A and B components, and there is a problem in discriminating the two. Some directional behaviour (Fig. 10) is considered to be an interplay of the A and B remanences. In this case the A remanence occupies the low to intermediate blocking temperature range and is resident in magnetite (see also Fig. 14a), while component B is reasonably identified above 580 °C and carried by hematite. As argued below, component A is considered to be the oldest remanence, and so in this case remanence acquisition of the B component was most likely facilitated via thermochemical processes (oxidation of magnetite), thereby producing apparent blocking-temperatures exceeding the older remanences. As for the A component, the B remanence may show a dual polarity structure at specimen level, and component separation can prove difficult. At least three components are idicated from Fig. 11, two of which show a dual polarity interplay of the B remanence with incomplete coercivity spectra separation, though the reverse field direction is considered to be isolated above 40–50 mT.

At some sites the distribution of characteristic remanence components tends to be smeared along great circles. For example, at site 69 on the western primary contact, red sandstone and neptunian dykes show A (confined to the neptunian dykes) and B remanences (Fig. 12a; mean values shown as stars), whereas the directional distribution of substrate (greenstones) sample-directions are quite extraordinary. High-temperature (HT) components can be reasonably defined above 550–660 °C, attended by discrete unblocking (Fig. 12c), but may show pronounced off-origin traces (Fig. 12b) when viewed in orthogonal vector projections. The latter may have originated via viscous behaviour/instrumental noise. The low–intermediate blocking spectra indicate the removal of 'antiparallel' field directions, but in most instances this component is not very well defined. The apparent HT components are smeared along a great circle which is apparently linked with the B remanence recorded from sandstones and Neptunian dykes. Similar features were noted at several sites, *all* located near the margins of the Massif (i.e. sites 32–33 & 69 (basement) and site 35 (Devonian)), and the great-circle trends (tested in *in situ* and stepwise unfolded coordinates) indicate smeared B remanences. These *apparent* and intermediate remanences may have originated through, e.g., magnetostatic coupling (Bailey & Hale 1981; Walderhaug & Torsvik 1987), transitional spot reading during field-reversal or alternatively strain-effects. The latter were carefully examined as these features are preferentially seen in sites along the margins, and can possibly explain data from sites

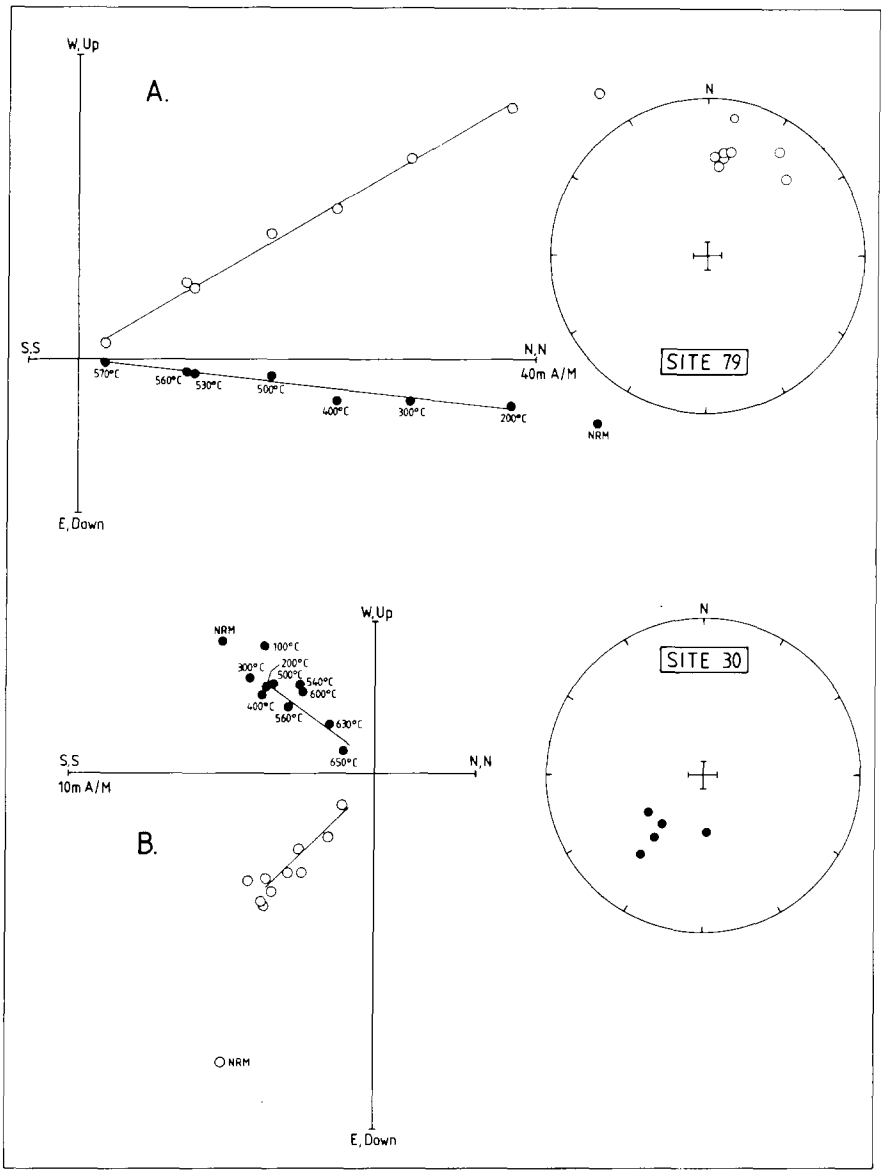

Fig. 8. Examples of thermal demagnetization from Devonian samples. (**A**) shows a well-defined single component A remanence, whereas (**B**) displays a somewhat more irregular decay pattern which is characteristic of the investigated samples. Corresponding stereoplots show the distribution of characteristic remanence components (sites 79 and 30). In stereoplots open or closed symbols, respectively, represent upward- or downward-pointing remanences. In vector diagrams open or closed symbols, respectively, represent points in the vertical or horizontal plane.

32–33. At site 69 such effects appear unlikely as no differences in the axial ratios or the direction of the principal axes from different specimens can be observed. The great circle, however, as defined by the characteristic remanence components, is close to the magnetic foliation plane with anisotropies as high as 20% (cf. Figs 2 & 3).

The interpretation of palaeomagnetic data can involve a certain amount of subjectivity. To illustrate a particular problem in the interpretation of the Hornelen data, site 34 is chosen as an interesting example (Fig. 2). Sampling embraces a steeply-dipping siltstone bed, showing a large number of small fault offsets of less than 0.5 m, striking almost parallel to the northern marginal fault. All tested samples show *single-component* magnetizations with distributed unblocking (Fig. 13). The within-site distribution indicates a cluster of north-westerly and steeply upward-pointing remanences, but the lack of a dual-polarity structure is obvious when viewed in *in situ* coordinates. The *in situ* distribution of the three northerly and steeply downward-pointing remanences, encircled in Fig. 13, may intuitively be considered as the B component, but *all* samples from this site show single-component remanences and identical blocking spectra below 580° (magnetite). When unfolding the bed, a dual-polarity structure emerges

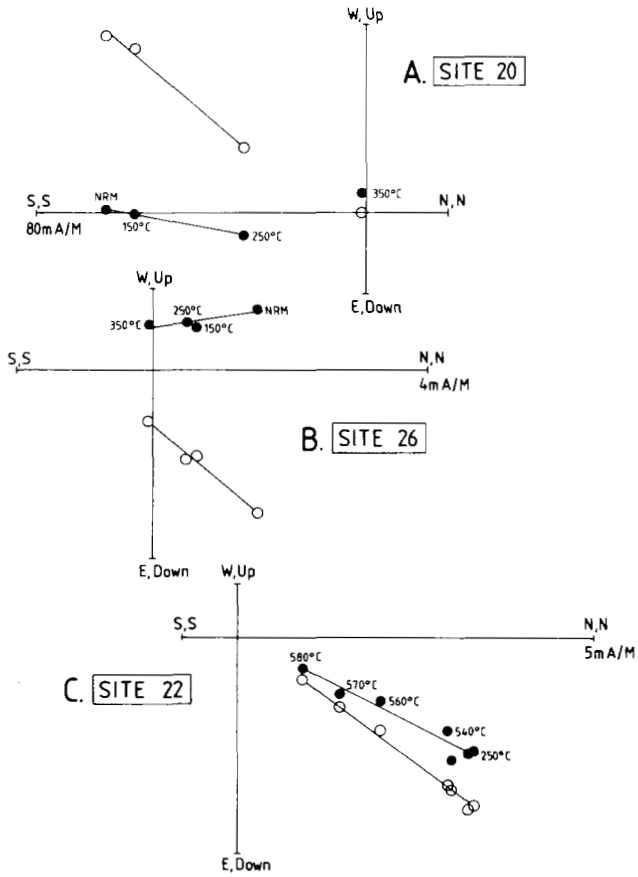

Fig. 9. (**A**) and (**B**): Examples of the B remanence occupying the low blocking temperature spectra for a basement (**A**, site 20) and a Devonian (**B**, site 26) sample. The high-temperature component was not established due to pronounced viscous behaviour above 250 and 350 °C, respectively. (**C**) a Devonian sample (site 22) where the B component appears to be the only one present (single component). Open and closed symbols have the same meanings as in Fig. 8.

which may relate to the A component, but with no difference in the blocking spectra. If so, however, the declination is plainly anomalous when compared with the bulk of tested sites (cf. Fig. 15). An explanation in terms of syn-fold remanence acquisition (blocked at various stages?) and subsequently affected by a *c.* 45° local anticlockwise rotation related to the minor fault offsets could perhaps explain the directional data from this site. From the Devonian the magnetic foliations/bedding are oblique to the marginal faults, but as noted in the magnetic fabric section (cf. Fig. 2), sites near the northern marginal fault are substantially fault-orientated, *apart from site 34*, which may represent a local post-faulting rotation. Since there are uncertainties regarding the interpretation of data from this site, the data have been left unexplained in Table 1 and have not been used in the final statistics.

Remanence analysis and fold-tests

Site mean-values (Fig. 15b, Table 1) were calculated from sites with reasonably well defined directional clusters/subclusters. Note though that α_{95} may be high, and may include only two sample-directions if these are the only ones recognized and are internally consistent. In cases where both normal and reverse field directions were present, the mean direction has been expressed in terms of the dominant polarity.

The distribution of site mean-values (Fig. 15b) from relatively well-defined locations indicates a reasonable pattern of the shallow–intermediate inclined A component and the more steeply inclined, dual-polarity structured B component. From the pre-Devonian substrate, component A has only been identified at site 25 (Torsvik *et al.* 1987*a*), and not used in the final statistics in the present account, whereas component B characterizes the substrate close to the margins of the Hornelen Massif. Two of the Devonian sites (1 & 82) are somewhat anomalous in both *in situ* and tectonic corrected coordinates, and define an almost sub-horizontal magnetization near NW–SE. The origin and

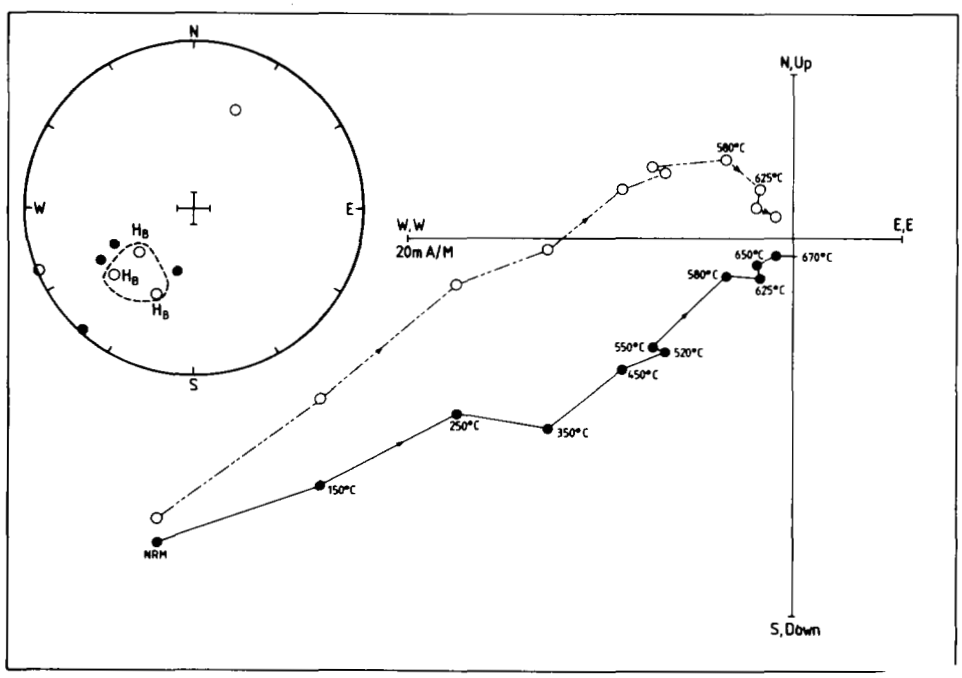

Fig. 10. Example of thermal demagnetization of a Devonian specimen from site 78 interpreted as an interplay of the A and B components. The B remanence occupies the high-temperature range, thus indicating a thermochemical origin. Stereoplot shows the characteristic remanence components for site 78, indicating the pattern of the upward-pointing B remanences and the downward-pointing A remanences, which at this site reside in T_b below 580 °C. Open and closed symbols have the same meanings as in Fig. 8.

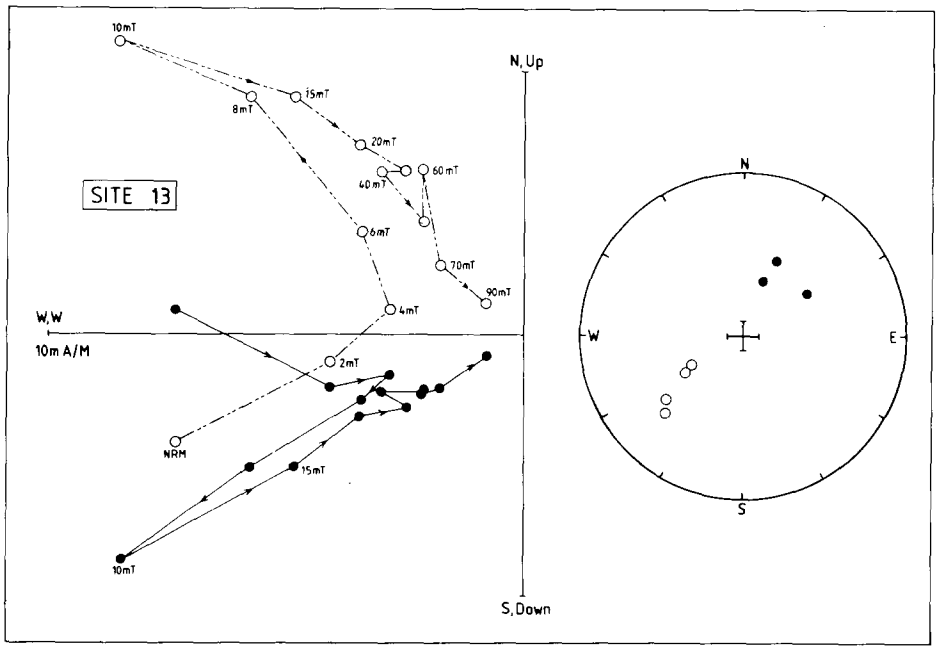

Fig. 11. Examples of a dual-polarity structured B remanence at sample level, and the distribution of characteristic remanence components for the site (site 13). Symbols have the same meanings as in Fig. 8.

significance of this remanence component is uncertain and there is no evidence for local tectonics as the bedding and magnetic foliation conform to the regional pattern (Fig. 2). In addition, a shallow inclined and almost sub-horizontal remanence observed from site 80 has not been included in the final fold-tests given below, since it represents a low blocking temperature component ($T_b < 250\,°C$) superimposed on and co-existing with the typical SW–NE A component (Table 1). We would stress, however, that the removal of these data has no important bearing on the following discussion.

The remaining 32 Devonian site-mean data were stepwise unfolded. Component B provides a negative fold-test at a high statistical confidence level, and post-dates folding of the Devonian rocks. *In situ* directions closely correspond to directional data obtained from the basement. With respect to the A component, different tectonic structures in the Devonian were examined by fold-tests. Most structures indicate a late syn-tectonic origin for the remanence, though this in some instances approaches the statistical limits (95% confidence level) in a conventional fold-test. This is summarized and illustrated in Fig. 16 where

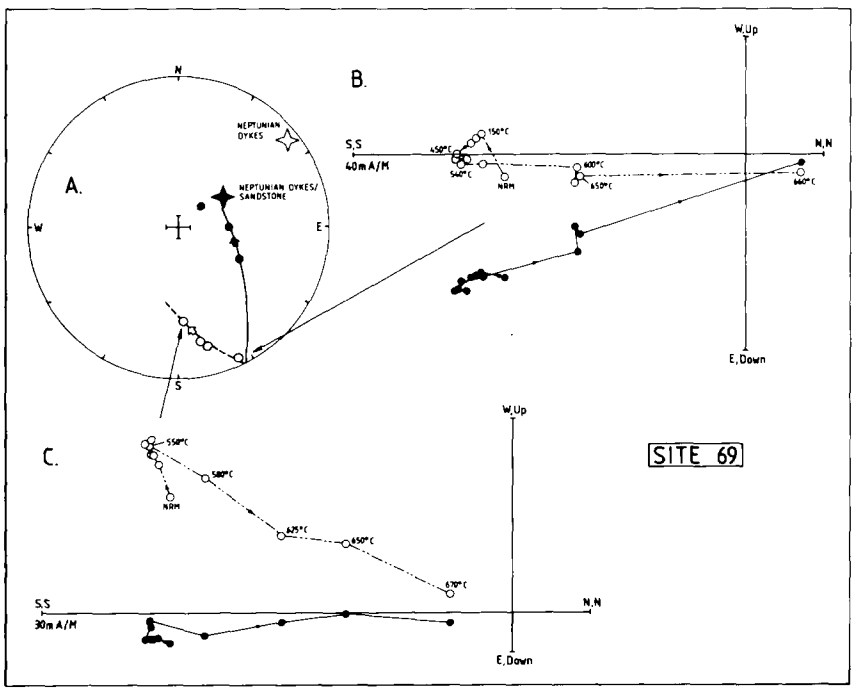

Fig. 12. (**A**) Distribution of high-T_b characteristic remanence components from basement samples at site 69, plotted with mean values from the overlying sandstone and interfringing neptunian dykes. Examples of thermal demagnetization of basement samples are shown in (**B**) and (**C**). Note that the apparent distribution of characteristic remanence components is smeared along a great circle which would intersect with the B component observed in neptunian dykes and sandstones (see text). Symbols have the same meanings as in Fig. 8.

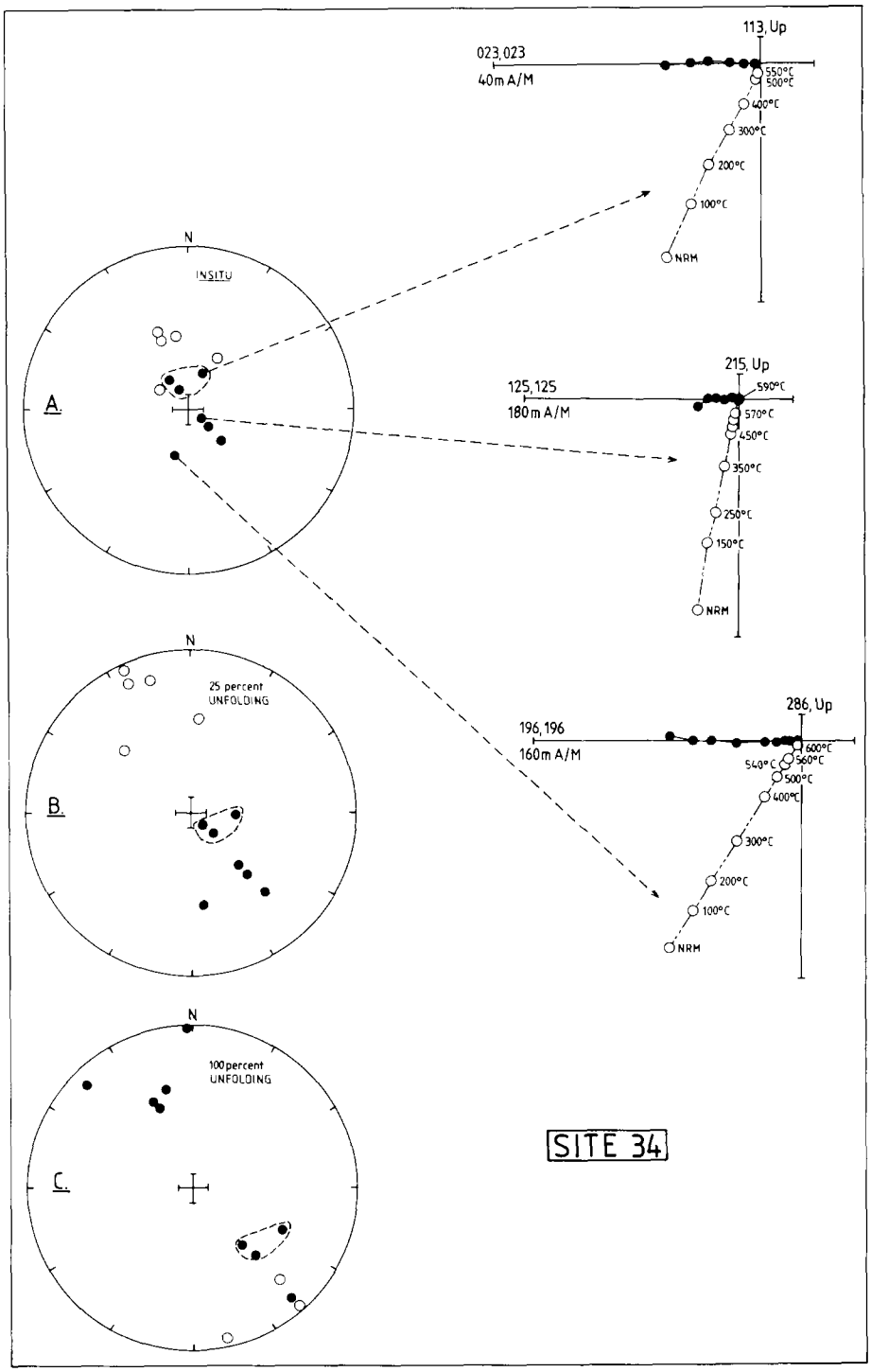

Fig. 13. Distribution of characteristic remanence components and examples of thermal demagnetization of site 34 specimens. (**B**) and (**C**) show partial (25%) and complete unfolding of the sampled bed (see text). Symbols have the same meanings as in Fig. 8.

normal, reversed and combined $(N + R)$ data indicate the late syn-tectonic nature of the A component. The most successful directional grouping and dual-polarity structure is accomplished by an overall 20% unfolding of the Devonian sediments. Note that the subdivision of normal and reverse is not strictly correct since a number of the sites have a dual polarity structure, and they are classified according to the dominant polarity (cf. Table 1). Normal polarity data may indicate a somewhat shallower inclination than the reverse field-component (Fig. 16d). This difference in inclination almost vanishes, however, if we analyse the data at sample level or separate mixed-polarity data, and must therefore be considered as partly an artefact of our manner of elucidating the remanence data. A conclusive magnetostratigraphic pattern for the Hornelen Massif could be taken as evidence for a primary syn-sedimentary origin of remanence. Such a pattern, however, is ambiguous and complicated by the presence of mixed-polarity sites. No systematic relationship of the A component and stratigraphy can be established (Fig. 17).

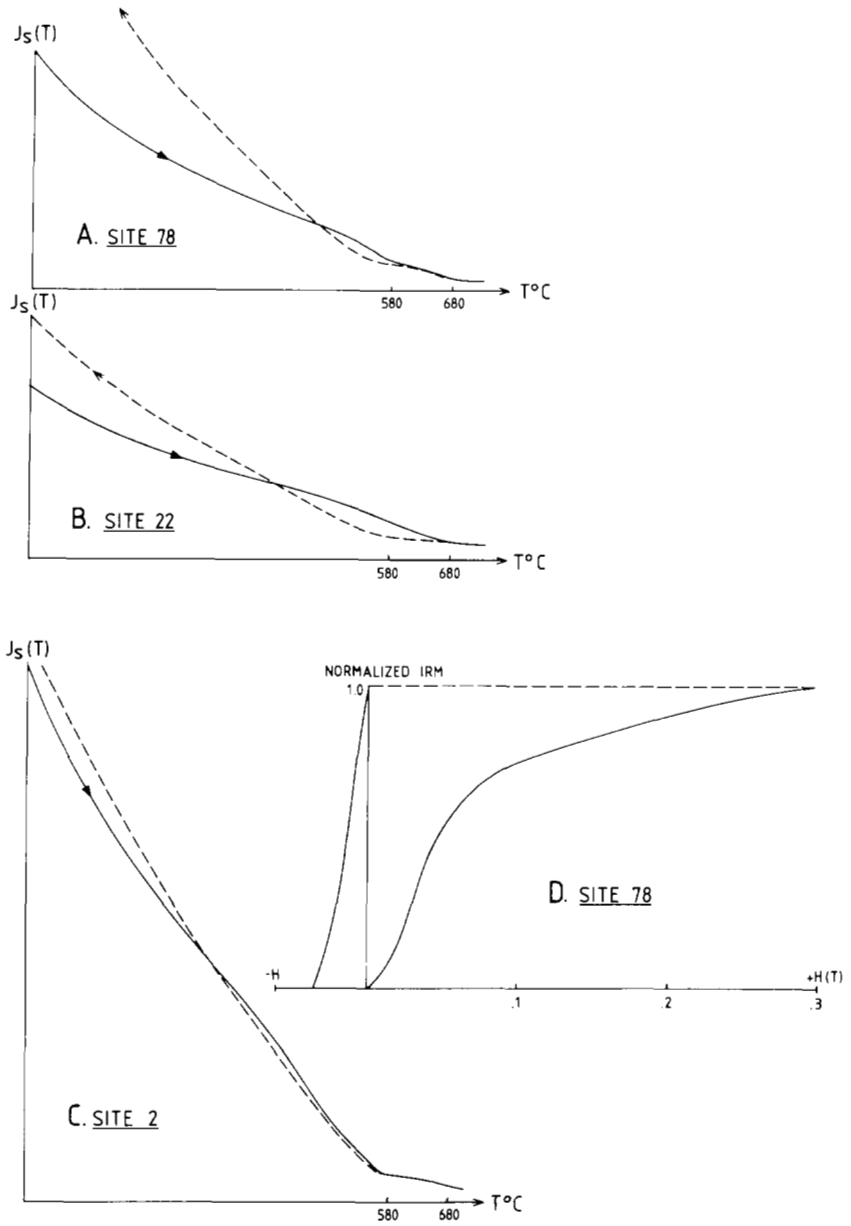

Fig. 14. Typical thermomagnetic (**A**)–(**C**), and isothermal (**D**) remanent acquisition curves for Devonian samples.

Discussion

The prelude to formation of the Lower to Middle Devonian basins was a comprehensive phase of late Silurian (Scandian) crustal imbrication and orogenesis (Fig. 18c, Phase 1). In the western part of the Norwegian Caledonides high P–T conditions during Scandian reconstitution are reflected in the formation of eclogites, yielding radiometric ages of *c.* 425 Ma (Bryhni & Andreasson 1985; Griffin *et al.* 1985).

The popular view of the Devonian of western Norway is one of a post-orogenic molasse deposited in fault-generated basins, and displaying a tectonic fabric acquired during late Solundian deformation (cf. Roberts 1983; Steel *et al.* 1985). A novel and extravagant approach has appealed to extensional tectonics and listric normal faults reactivating former Scandian thrust zones (Fig. 18c, Phase 2) to create the Devonian basins (Hossack 1984). This model incorporated some of the structural features, e.g. large folds, into this phase of activity, and the E–W cross-faults we can clearly discern were thought to have functioned as lateral ramps. In such a model the folds which developed in the basins were accommodation structures to the lateral ramps.

Magnetic and structural fabrics from the Hornelen Massif and its substrate reveal folding on E–W axes. The Devonian sediments are essentially folded into a large open syncline while the more anisotropic substrate displays a sequence of smaller and tighter folds (Fig. 19a). The predominant foliation in the metamorphic rocks of the basement, locally mylonitic, is essentially Scandian in age, so that the marked truncation of basement structures and the angularity of the unconformity is a consequence of deep pre-Devonian erosion. In the Håsteinen area to the south (cf. Fig. 1b), Solundian deformation is more profound with noncylindrical E–W folds plunging up to 70°. The magnetic

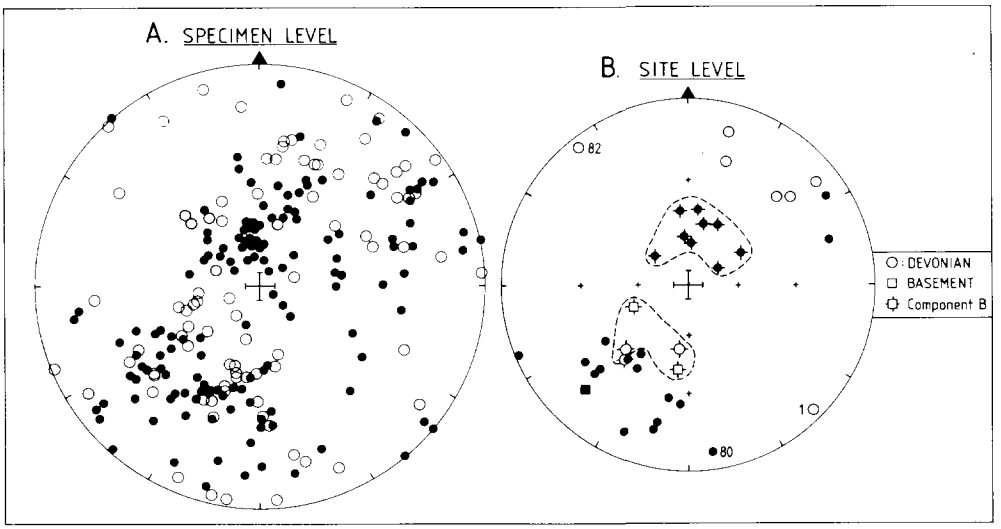

Fig. 15. Distribution of all identified characteristic remanence components at specimen level (**A**), including anomalous data not used in the final analysis, and site-mean values for Devonian sites and the substrate (**B**); cf. Table 1 and text. Open symbols are up.

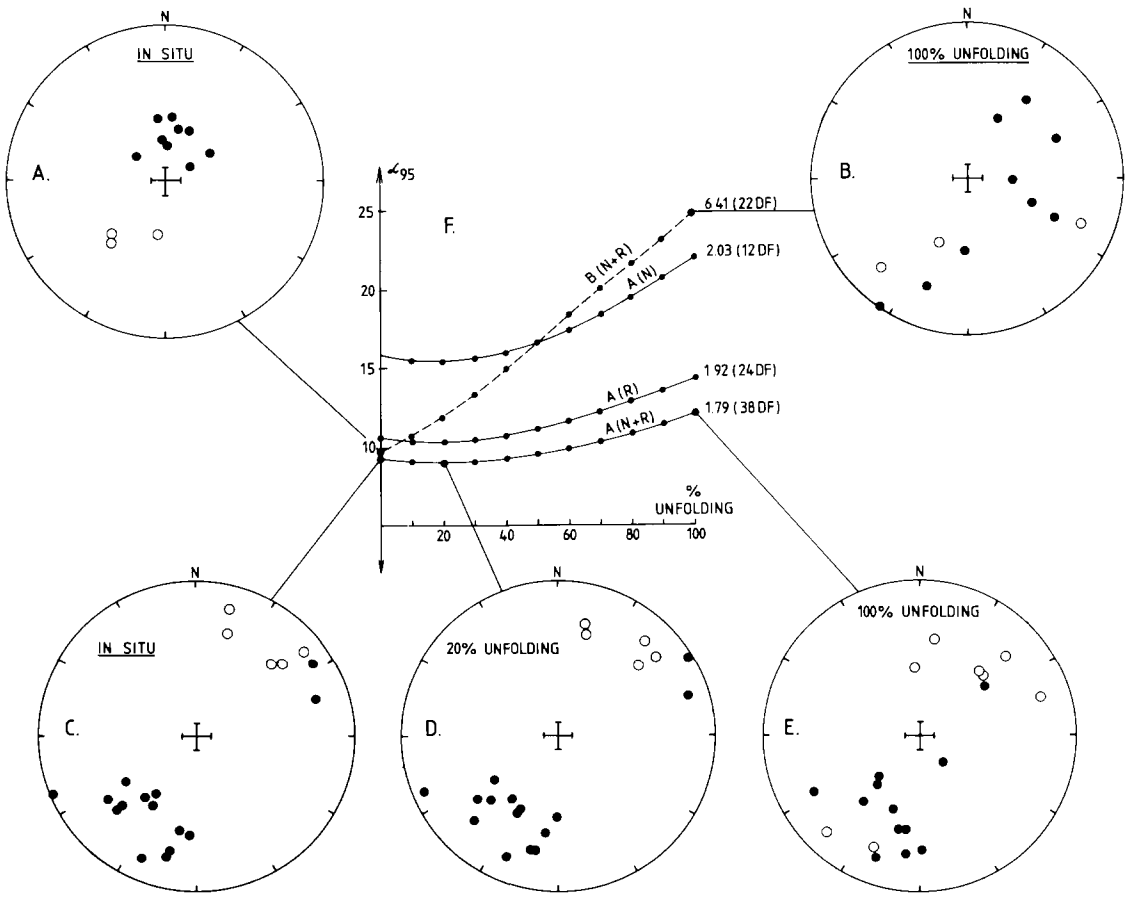

Fig. 16. Fold test for Devonian sites. (**A**), (**B**) show Group B remanences in *in situ* and the 100% unfolding state; a post-fold origin is clearly indicated. (**C**), (**D**) & (**E**) show the A component in *in situ*, partial (20%) and total unfolding state. This latter test indicates a syn-fold origin of remanence, though the statistical significance is arguable. Note that to the right of each curve, k ratios are given along with the degrees of freedom. Open symbols are up. In (**F**) the response in α_{95} to unfolding has been shown for the A data combined and separated (normal/reverse). The B component is a combined test of normal/reverse sites.

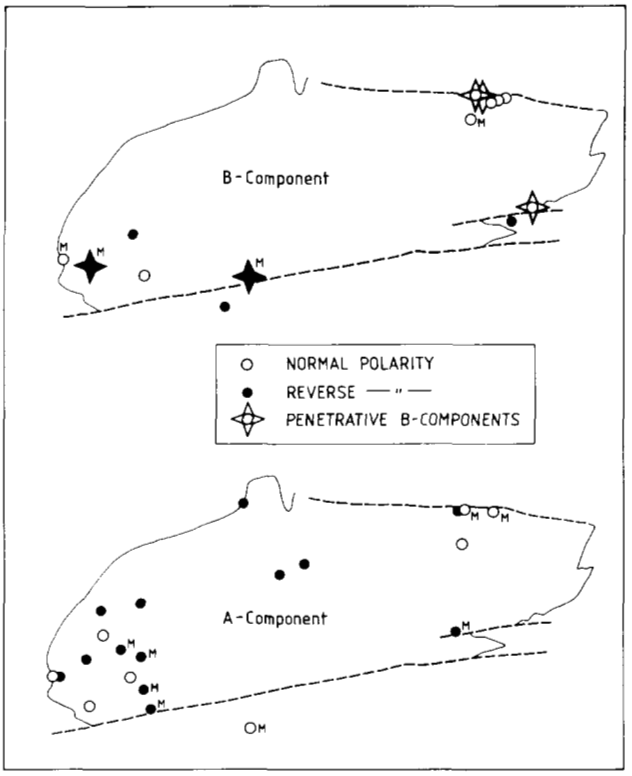

Fig. 17. Areal distribution of the B and A components. (see text). Continuous and broken lines indicate boundary of Hornelen Massif.

fabrics in *this* massif mirror the axial plane structures of both the Devonian rocks and their substrate (Torsvik *et al.* 1987*a*). Folding of the Hornelen Massif, on the other hand, was only occasionally attended by development of an axial-plane cleavage. The magnetic foliation is substantially bedding-orientated (Fig. 5), but there are possible indications that the magnetic foliation and occasional examples of megascopic cleavage may relate to a tectonic event prior to folding, but this remains to be proved in future studies. The strong easterly plunging, fold axis-parallel magnetic lineation, congruous with the substrate lineations, could also, at least partly, be of tectonic origin. This lineation is notably more consistent than linear palaeocurrent indicators, but problems remain in discriminating between possible primary and tectonic induced linear fabrics.

Apart from some marginal sites (26–34) where the magnetic fabrics have an obviously post-fold origin, the structural elements (bedding/cleavage) of the Hornelen Devonian sediments are sharply truncated by the present marginal faults, particularly marked along the southern boundary of the Massif. This is readily seen in Fig. 2. The bedding and fault relationships from the NE part of the Massif (Fig. 19b) clearly demonstrate that syn-depositional normal-faulting at the site of the present northern marginal faults is at best unlikely. It is commonly assumed that the Hornelen 'Basin' is continuously fringed by coarse alluvial fan deposits, and indeed virtually all modern maps show this (see also Fig. 1b). Along both the southern and northern margins a number of sandstone horizons (up to several hundred metres in outcrop width) strike into the marginal faults where they are brutally truncated, thus showing that the present faults in fact truncate both facies boundaries and the fold-pattern. As the marginal faults cross-cut the structural fabrics, facies belts and zones of potential weakess, it could be envisaged that they may have originally developed as strike-slip faults. Judging from the fold pattern in the north-western part of the Massif and the apparent change of NNE- to E–W-striking megascopic foliations (flexuring?) in the gneisses, we raise the possibility that this marginal fault originated via sinistral slip on an S-shaped fault trajectory, thus producing contraction in the NW part of the Massif.

The tectonothermal features of the Devonian and its substrate, i.e. folding, cleavage, lineations, data on illite crystallinity and magnetic properties point to N–S crustal compression, under temperatures of anchizonal to lower greenschist facies metamorphism (Vogt 1928; Nilsen 1968; Roberts 1983; Steel *et al.* 1985; Torsvik *et al.* 1986, 1987*a*; Ramsay *et al.* 1987). The A magnetization obtained from the Hornelen Massif (Table 2) is considered to be of essentially secondary origin, related to burial with only modest internal deformation, and promoted by a combination of thermo-viscous (TVRM) and thermo-chemical (TCRM) processes at temperatures probably above 350–400 °C. Fold-tests indicate that major remanence acquisition was completed prior to the final stages of folding (*c.* 80% folding), indicating a syn-fold origin of the remanence induced during crustal uplift in a palaeofield of varying polarity. Some of the remanence complexity in the Hornelen Massif, however, may possibly be ascribed to the presence of primary remnants, although we have found no unambiguous evidence for this.

The Apparent Polar Wander (APW) path for Fennoscandia and the palaeolatitudinal implications as outlined in Figs 18a & b (based on Pesonen *et al.* 1987; cf. Table 3) is employed merely as a working model. The relative pole-position obtained from the Devonian rocks of Kvamshesten, Håsteinen and Hornelen ORS (A components) and their substrates form a polar group around 15 °N, 150 °E (Fig. 19a), suggesting a late Devonian/early Carboniferous age. These data are thought to reflect magnetic resetting during the crustal uplift history of the Svalbardian (Solundian) Orogeny (Fig. 18c, Phase 3), and apparently conform to an $^{39}Ar/^{40}Ar$ (biotite) age of 375 Ma obtained from Stadlandet (Lux 1985), and other similar biotite (K-Ar) ages from Western Norway.

High-blocking remanence components recorded in the Upper Silurian/Lower Devonian Ringerike ORS have been argued as pre-dating folding in the Oslo area (at least pre-Middle Carboniferous), and considered to be of a primary nature (Douglass 1987). Incidentally, the Ringerike pole partly overlaps with the Håsteinen pole (Fig. 18a), though its overall more easterly pole position compared with the bulk of Western Devonian ORS may indicate real time differences and, if correct, implies (1) insignificant APW for Fennoscandia (or alternatively complete magnetic resetting of the Ringerike ORS prior to folding) in the Late Silurian–Late Devonian (or Early Carboniferous) range, and (2) that Svalbardian deformation and subsequent magnetic resetting was most profound in western Norway.

Important episodes of Mesozoic extensional tectonics, partly guided by Solundian and Scandian structures, are recognized throughout the length of western and central Norway, and are most likely important controlling elements in the structural and basinal evolution offshore western

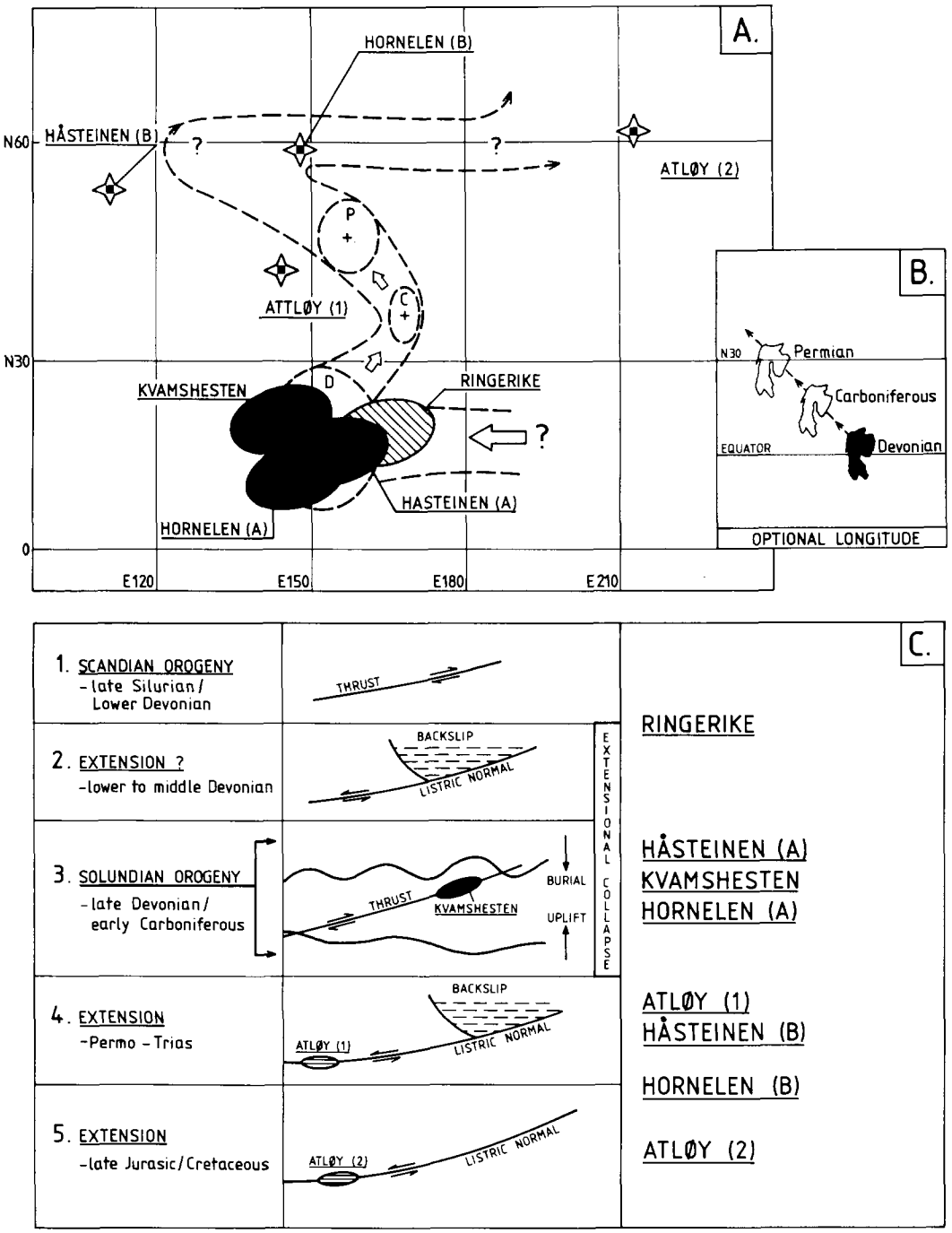

Fig. 18. (**A**) Selected pole positions (cf. Discussion) displayed on a provisional apparent polar wander path given in Pesonen *et al.* (1987); cf. also Sturt & Torsvik (1987), with A_{95} confidence limits. D, C and P denote the mean Devonian, Carboniferous and Permian pole positions obtained from Fennoscandian data. The Devonian massifs, partly including substrate, of Kvamshesten, Håsteinen, Hornelen and Ringerike ORS are shown with d_p and d_m semi-axes, whereas Late Palaeozoic/Mesozoic poles are shown as stars. (**B**) The latitudinal position of Fennoscandia with respect to mean poles D, C and P in (**A**). (**C**) A generalized tectonic model of the Western Norwegian Caledonides linking events with the recent palaeomagnetic findings (see text). Names stated on the right in the figure refer to poles shown in (A), and they are listed vertically in a proposed age pattern. Table 3 provides information concerning all these poles. The events portrayed in (**C**) are observed in the Kvamshesten ORS. An early phase of folding of the ORS is associated with burial to a considerable depth. Later thrusting (Dalsfjord Fault) and a second phase of folding are associated with uplift of the ORS.

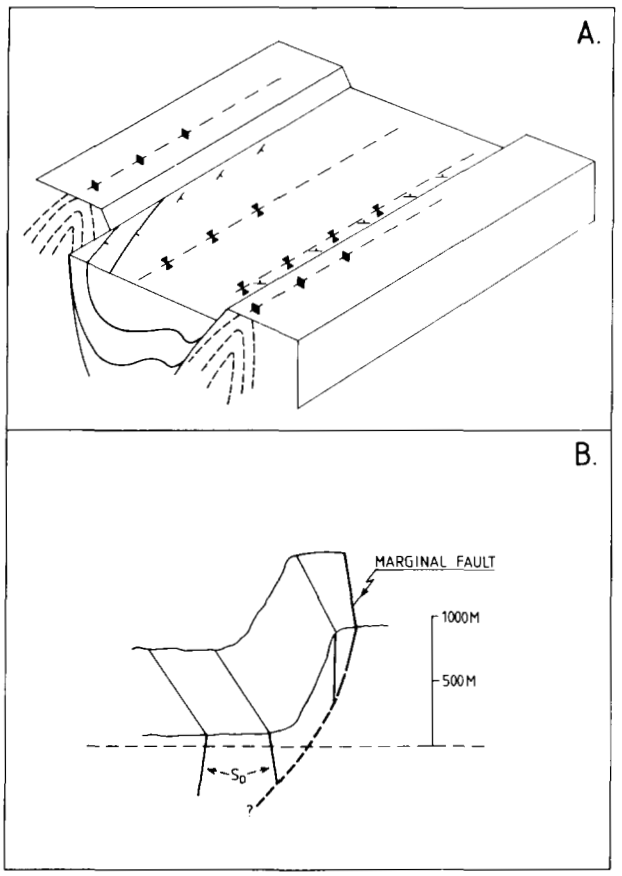

Fig. 19. (**A**) simplified model for the structural setting of the Hornelen Massif, i.e. folding and later normal faulting at the present fault margins. (**B**) a typical bedding/fault relationship in the NE part of the Massif. The profile corresponds to a section embracing sites 5 & 6 to 28/29.

Norway. From the Hornelen Massif, the present marginal faults truncate a regional megascopic fold belt. It is evident, from the present data base, that the signature of the B component is not basin-wide (Fig. 17) and is most profoundly developed along the marginal faults and the primary uncorformity in the south-western part of the Massif. The B component is notably 'penetrative' in sites close to the margins (Fig. 17), although other sites along the margin (e.g. site 67) show no definite evidence for this B component. The B component has its origin partly via thermochemical processes, since it may co-exist and be resident in apparent blocking temperatures exceeding those of the older A component. In terms of a directly tectonically linked origin, the B component near the marginal fault may have been acquired via brittle shear and fluid circulation in the fault zone, whereas subordinate and localized shears relating to marginal fault movements along the western primary unconformity may have been of importance. Along the primary unconformity, however, there are important E–W subordinate offset faults (cf. Larsen *et al.* 1981). It is suggested that the Hornelen B component brackets a *minimum* age and duration of important fault activity, as intra-Jurassic (Fig. 18a). A partly developed, late uplift-related magnetization cannot be excluded, although this would be expected to have a more widely developed overprint. Analogously, the Håsteinen ORS (Torsvik *et al.* 1987*a*) and the Kvamshesten ORS with its basal mylonites bear the signature of the Solundian Orogeny (Table 3, Fig. 18a & c). Palaeomagnetic data from shears, in part ductile, operating on the Western primary unconformity of the Håsteinen Massif (Håsteinen B component in Fig. 18a) indicate a Triassic/early Jurassic age, while important post-Devonian dip-slip movement is indicated along the south-western part of the Dalsfjord Fault (Atløy; see Fig. 1b). These normal fault movements are indicated by the development of two distinct phases of fault brecciation (Fig. 18c, Phases 4 & 5), for which palaeomagnetic data suggest a Permo-Triassic age (Sturt & Torsvik 1986), and a younger phase of brittle reactivation on the Dalsfjord Fault probably during Jurassic–Early Cretaceous times.

Conclusion

Palaeomagnetic and structural data indicate that the evolution of the Devonian rocks of western Norway contains a variety of structural elements produced over a

Table 3. *Unrefined, magnetic age classification of some selected palaeomagnetic pole-positions discussed in the text and shown in Fig. 18*

	Silurian [*Scandian*]	Devonian [*Solundian*]	Carbonif.	Permian	Mesozoic
KH (mD)[1]		[N21 E144]			
HÅ (mD)		[N16 E155]			[N54 E111]
HO (mD)		[N12 E147]			[N59 E148]
DFA				[N43 E144]	[N61 E213]
Rs (uS/lD)	[N19 E164]				
Mean poles:					
D		[N18 E152]			
C			[N37 E168]		
P				[N48 E157]	

KH, Kvamshesten ORS & Dalsfjord Mylonites (Torsvik *et al.* 1986); HÅ, Håsteinen ORS & substrata (Torsvik *et al.* 1987*a*); HO, Hornelen ORS & substrata (present study); DFA, Dalsfjord Fault Atløy (Sturt & Torsvik 1986); RS, Ringerike Sandstone (Douglass 1987); D, C & P, mean poles cited in Pesonen *et al.* (1987), and also detailed in Sturt & Torsvik (1987).

[1] Depositional ages inferred from plant/fish fossils: D, Devonian; S, Silurian; l, lower; m, middle; u, upper.

considerable time span. An understanding of the tectonic setting of the West Norwegian Devonian massifs must involve the ability to differentiate between (1) Scandian crustal deformation and imbrication, (2) basinal formation, (3) the Solundian Orogeny (the A components), and (4) & (5) those structures and remanences (the B components) promoted by extensive Mesozoic faulting and reactivation (Fig. 19). So far, in much of the modern literature important late Devonian (Soloundian), Mesozoic and as yet unverified structures have been blended together as elements in sedimentary models for the origin of the Devonian Massifs, and integrated by some into a single kinematic event to explain their deformation. The sedimentary and tectonic setting(s) relating to the formation of the western Norwegian Devonian is still an open question. This account does *not* attempt to shed any new light on this issue, but merely points out that some 'basinal' marginal faults, required by a number of the published models for the evolution of the Devonian, are in fact late structures, some of Mesozoic origin. We draw the reader's attention to (1) the fact that the present marginal faults of the Hornelen Massif were not the sites of Devonian oblique-slip movements, nor could they have represented lateral ramps in an extensional collapse model, and (2) that the sum of the various lines of evidence would require that the megascopic fold-patterns and other deformational features are elements of a compressional and post-depositional tectonic framework. This, however, does not imply that tectonic controls on Devonian sedimentation were unimportant, but we consider that the precise nature of the syn-depositional tectonic framework cannot be predicted from the faults now observed to cut these Devonian rocks. These faults appear to have had their origin in latest Palaeozoic and Mesozoic extensional deformation, and we submit that the graben-like form of the Hornelen Massif is essentially one of Mesozoic construction.

The authors are grateful to Elf Aquitaine Norge for valuable financial support and THT also acknowledges the Norwegian Research Council for the Humanities and Science for financial support (grant D. 41.12.021). Improvements of the manuscript by D. H. Tarling and A. Boyle are greatly appreciated. The figures were prepared in the drawing office of the Norwegian Geological Survey. Norwegian Lithosphere Contribution 22.

References

BAILEY, M. E. & HALE, C. J. 1981. Anomalous magnetic directions recorded by laboratory-induced chemical remanent magnetization. *Nature*, **294**, 739–41.

BRYHNI, I. 1964. Migrating basins on the Old Red Continent. *Nature*, **202**, 384–5.

—— 1966. Reconnaissance Studies of Gneisses, Ultrabasites, Eclogites and Anorthosites in outer Nordfjord, Western Norway. *Norges Geologiske Undersøkelse*, **241**, 1–68.

—— 1978. Flood deposits in the Hornelen Basin, West Norway (Old Red Sandstone). *Norske Geologiske Tidsskrift*, **58**, 273–300.

—— & ANDREASSON, P. G. 1985. Metamorphism in the Scandinavian Caledonides. *In*: GEE, D. G. & STURT, B. A. (eds) *The Caledonide Orogen—Scandinavia and Related Areas*. John Wiley, New York, 763–81.

DOUGLASS, D. N. 1987. Palaeomagnetics of Ringerike Old Red Sandstone and related rocks, Southern Norway; implications for large separation of Baltica and British Terranes. *Tectonophysics* (submitted).

FISHER, R. A. 1953. Dispersion on a sphere *Proceedings of the Royal Society, London* Series A, **217**, 295–305.

GRIFFIN, W. L., AUSTRHEIM, H., BRASTAD, K., BRYHNI, I., KRILL, A. G., KROGH, E. J., MARK, M. B. E., QVALE, H. & TRUDBAKKEN, B. 1985. High-pressure metamorphism in the Scandinavian Caledonides. *In*: GEE, D. G. & STURT, B. A. (eds) *The Caledonide Orogen–Scandinavia and Related Areas*. John Wiley, New York, 783–801.

London, **141**, 629–32.

KENT, J. T., BRIDEN, J. C. & MARDIA, K. V. 1983. Linear and planar structure in ordered multivariate data as applied to progressive demagnetization of palaeomagnetic remanence. *Geophysical Journal of the Royal Astronomical Society*, **75**, 593–621.

KOLDERUP, C. F. 1926. Solunds Devonfelt (English summary). *Bergens Mus. Aarbok 1924–25, Naturv. Rekke*, **11**, 1–23.

LARSEN, V., SPINNANGER, A., STEEL, R., AASHEIM, S., GLOPPEN, T. G. & MAHLE, S. 1981. *A field guide to Hornelen Basin—a deep, late-orogenic basin (Devonian) in Western Norway*. Inter. Publication, University of Bergen (Statoil), Norway.

LUX, D. R. 1985. K/Ar ages from the Basal gneiss region, Stadtlandet area, western Norway. *Norske Geologiske Tidskrift*, **65**, 277.

MIKKELSEN, J. 1986. *Field data and regional speculations, Sogn, Western Norway*. Field guide, Internal Publication, University of Bergen, Geological Institute, Bergen, Norway.

NILSEN, T. H. 1968. The relationship of sedimentation to tectonics in the Solund Devonian district of Southwestern Norway. *Norges Geologiske Undersøkelse*, **259**.

NORTON, M. G. 1986. Late Caledonian extension in Western Norway: A response to extreme crustal thickneing. *Tectonics*, **5**, 2, 195–204.

PESONEN, L., TORSVIK, T. H., BYLUND, G. & ELMING, S. Å. 1987. Crustal evolution of Fennoscandia—Palaeomagnetic constraints. *Tectonophysics* (in press).

RAMSAY, D. M., STURT, B. A., TORSVIK, T. H., KIRSCH, H. & BERING, D. 1987. The structural evolution of the Devonian sequence of Kvamshesten, Western Norway. *Terra Cognita* (abstract), **7**.

ROBERTS, D. 1983. Devonian tectonic deformation in the Norwegian Caledonides and its regional perspectives. *Norges Geologiske Undersøkelse*, **380**, 85–96.

STEEL, R. J. & GLOPPEN, T. G. 1980. Late Caledonian (Devonian) basin formation, western Norway: sign of strike-slip tectonics during infilling. *Special Publication, International Association of Sedimentologists*, **4**, 79–103.

——, SIEDLECKA, A. & ROBERTS, D. 1985. The Old Red Sandstone basins in Norway and their deformation: A review. *In*: GEE, D. & STURT, B. A. (eds) *The Caledonide Orogen: Scandinavia and Related Areas*. John Wiley, New York, 293–315.

STURT, B. A. & TORSVIK, T. H. 1986. Palaeomagnetism and dating of fault movements (abstract). Paper presented at the *17th Nordic Geology Meeting*, Helsinki.

—— & —— 1987. A late Carboniferous palaeomagnetic pole recorded from a Syenite sill, Stabben, Central Norway. *Physics of the Earth and Planetary Interiors*, **49**, 350–9.

TORSVIK, T. H. 1986. *IAPD—Interactive Analysis of Palaeomagnetic Data (User-guide and program description)*. Internal Publication, University of Bergen, Institute of Geophysics, Bergen, Norway.

——, STURT, B. A., RAMSAY, D. M., KISCH, H. J. & BERING, D. 1986. The tectonic implications of Solundian (Upper Devonian) magnetization of the Devonian rocks of Kvamshesten, western Norway. *Earth and Planetary Science Letters*, **80**, 337–47.

——, ——, —— & VETTI, V. 1987*a*. The tectono-magnetic signature of the Old Red Sandstone and Pre-Devonian strata in the Håsteinen area, Western Norway, and implications for the later stages of the Caledonian Orogeny. *Tectonics*, **6**, 3, 305–22.

——, HOLME, J., STURT, B. A., RAMSAY, D. & BERING, D. 1987*b*. The magnetic fabrics of the Solund Massif, Western Norway (in preparation).

VOGT, T. 1928. Den norske fjellkjedens revolusjonsshistorie. *Norges Geologiske Undersøkelse*, **122**, 97–115.

WALDERHAUG, H. J. & TORSVIK, T. H. 1987. TRM and TCRM laboratory experiments and their palaeomagnetic implications. *Terra Cognita* (abstract), **7**, 472.

Received 6 May 1987; revised typescript accepted 22 September 1987.